Journal of ELECTRONIC MATERIALS, Vol. 44, No. 1, 2015
DOI: 10.1007/s11664-014-3514-6

Structural, Electrical, and Magnetic Properties of High-Temperature-Sintered $La_{1-x}Na_xMnO_3$ ($0.05 \le x \le 0.35$) Compounds

A.E. IRMAK,[1,2,4] E. TAŞARKUYU,[1,2] A. COŞKUN,[1,2] S. AKTÜRK,[1,2] Z. DIKMEN,[3] and Ö. ORHUN[3]

1.—Department of Physics, Faculty of Sciences, Mugla Sitki Kocman University, 48000 Mugla, Turkey. 2.—Magnetic Materials Laboratory, Research Laboratories Center, Mugla Sitki Kocman University, 48000 Mugla, Turkey. 3.—Department of Physics, Faculty of Sciences, Anadolu University, 26470 Eskişehir, Turkey. 4.—e-mail: ekberirmak@gmail.com

The structural, electric, and magnetic properties of $La_{1-x}Na_xMnO_3$ ($0.05 \le x \le 0.35$) compounds have been investigated. The compounds were prepared by a standard sol–gel method then sintered at 1400°C for 24 h. The crystal structures were orthorhombic (Pbnm) for all Na concentrations, and the unit cell volumes, determined from the x-ray diffraction data, tended to decrease with increasing Na content. The high-temperature-sintering process resulted in a grainy structure with grain sizes of 5–30 μm. The Curie temperature (T_C) increased with increasing Na concentration up to $x = 0.20$, then decreased with further increase in Na concentration. The maximum magnetic entropy change ($-\Delta S_M$) under a field change of 1.6 T was calculated to be ~3 J/kg K for the sample containing 15% Na.

Key words: Sintering temperature, impurity, concentration, magnetic properties, magnetic entropy

INTRODUCTION

The rare earth mixed-valence manganites with the general formula $R_{1-x}A_xMnO_3$ (where R is a rare earth cation, A is a divalent or monovalent doping cation, and x is the doping concentration) have been extensively studied in recent decades.[1–4] They have important technological applications, for example in magnetic cooling, hard disk read heads, fuel cells, and infrared devices, and as magnetic field sensor and micro-wave active components. These materials are known as perovskite manganites because of their crystal structure, which is the same as that of the mineral perovskite, $CaTiO_3$.

Lanthanum manganite ($LaMnO_3$), which is a member of this family, is anti-ferromagnetic and an insulator material. Substitution of a monovalent or a divalent element for La in $LaMnO_3$ makes the material ferromagnetic, and a conductor below its T_C.[5,6] On substitution of a monovalent or divalent ion for La^{3+} ion, some of the Mn^{3+} ions become Mn^{4+} ions, in proportion to the substituted ion concentration.[7] Co-existence of manganese in two valence states has a substantial effect on the physical properties of these materials. It has been shown that substitution by divalent elements in the range $0.30 \le x \le 0.40$ and by monovalent elements in the range $0.15 \le x \le 0.20$ results in materials with useful magnetic and electrical properties.[8,9] The explanation of this is that if the substituted ion is divalent, it oxidizes an Mn^{3+} ion to a Mn^{4+} ion, but if it is a monovalent ion, it oxidizes two Mn^{3+} ions to two Mn^{4+} ions. Therefore, the Mn^{4+}-to-Mn^{3+} ratio changes depending on the valence state and the concentration of the substituent ion. It is well known that Mn^{3+} and Mn^{4+} ions differ in ionic radii. La^{3+} and the substituent ion may also have different ionic radii. Because of these ionic radii differences, concentration is very important to the crystal structure of the resulting compound.[10–12]

(Received July 13, 2014; accepted November 1, 2014; published online December 2, 2014)

The ionic radius of the Mn^{4+} ion is smaller than that of Mn^{3+}. Distortion of the perovskite structure characterized by tilting of the MnO_6 octahedra occurs as a result of doping, with the tilting angle dependent on concentration. Depending on the changes in the Mn^{4+}-to-Mn^{3+} ratio that occur as a result of the substitution, the lattice constants, Mn–O bond angles, and Mn–O–Mn bond lengths change, which, in turn, has a positive or negative effect on the magnetic and the electrical properties.

$LaMnO_3$ compounds have the perovskite structure, the stability of which depends on the ionic radii of the species present in the La and Mn sites. To preserve the perovskite structure the ionic radius of the substituent element should be in a well-defined range. The Goldschmidt tolerance factor, t, a measure of lattice distortion, is given as: $t = \frac{r_A + r_O}{\sqrt{2}(r_B + r_O)}$ where, r_A and r_B are the mean ionic radii of the La and Mn sites and r_O is the radius of the O ion. For an ideal cubic lattice, t is equal to 1; as r_A decreases and when the substituent ion in the La site has different valence from 3+, r_B also decreases, hence t changes. If $t > 1$ the resulting structure will have hexagonal symmetry. If $0.86 < t < 1$ the structure is cubic, and if t is smaller than 0.86 the symmetry of the structure is reduced. Another structural property is the cation size mismatch, σ^2, a measure of the La site disorder of the structure. The cation size mismatch is defined as $\sigma^2 = \sum_i x_i r_i^2 - r_A^2$, where x_i is the concentration of the ion, r_i is the ionic radius of that ion, and r_A is the average ionic radius of the La site ions. If the La site of the compound is doped with an ion that has an ionic size different from that of La, distortion of the crystal structure occurs. This distortion leads to a different Mn–O bond distance and a deviation of the Mn–O–Mn bond angle from 180°. These changes in the structure of the compound can be controlled by doping with more than one ion with different ionic radii or with valence states other than 3+. By controlling the distortion of the structure of the compound, its electrical and magnetic properties can be manipulated.

Heat treatment is another important means of manipulating structure. It seems possible to improve desired physical properties by finding the appropriate heat-treatment process, in addition to the appropriate doping element and its concentration. Heat treatment can result in controlled growth of grains, leading to improvement of some physical properties.[13,14]

In this work, the effects of Na concentration and high sintering temperature (1400°C) on the structural, electrical, and magnetic properties of $La_{1-x}Na_xMnO_3$ (x = 0.05, 0.10, 0.15, 0.20, 0.25, 0.30, 0.35) compounds was studied.

EXPERIMENTAL

To obtain homogeneous mixtures, the $La_{1-x}Na_xMnO_3$ samples (x = 0.05, 0.10, 0.15, 0.20, 0.25, 0.30, 0.35) were prepared by the sol–gel method. Stoichiometric amounts of La_2O_3, Na_2CO_3 and $Mn(NO_3)_2$ were dissolved in dilute HNO_3 solution at 150°C. Citric acid and ethylene glycol were then added to the mixture and the homogeneous solution obtained was slowly boiled at 200°C, giving a viscous residue. This residue was dried slowly at 300°C until a dry gel was obtained. This was burned in air at 600°C to remove the organic materials produced during the chemical reactions. The material from this process was ground to obtain fine powder and then fired in air at 1000°C for 24 h. The product was re-ground and pressed into 13-mm pellets with 3 tons pressure and sintered in air at 1400°C for 24 h.

Scanning electron microscopy (SEM) was performed with a Jeol SEM 7000F. XRD data ($10° \le 2\theta \le 70°$) was obtained by use of a Bruker D8 Advance x-ray diffractometer with a $CuK\alpha_1$ radiation. Magnetic properties from 100 K to 320 K were investigated by use of a Lakeshore model 7304 vibrating sample magnetometer (VSM) with a closed-cycle helium cryostat and applied magnetic fields up to 1.6 T. From the temperature-dependence of magnetization, T_C was determined at an applied field of 100 Oe. Field-dependent magnetization measurements of the samples were obtained at temperatures in the region of T_C with 5 K intervals and the fields between 0 T and 1.6 T.

RESULTS AND DISCUSSION

The XRD patterns of the samples (Fig. 1) were indexed to an orthorhombic lattice with Pbnm space group. To investigate the effect of Na concentration, structural data were refined by use of Rietveld's profile-fitting method by use of the freely available FullProf suit software. The calculated lattice constants, unit cell volumes, and refinement data are presented in Table I. Samples with $x \ge 0.15$ contained a small volume fraction of MnO impurity with a cubic structure ($Fm\bar{3}$ m) (COD data base entry number 96-900-5947), which gave characteristic peaks near $2\theta = 40.50°$ and 58.61°, as marked in Fig. 1. As Na content increased the unit cell volume decreased for x up to 0.20; unit cell volume was then almost constant for further increases of Na content. This behavior has already been reported for sodium-doped manganites.[5] The increase in the average La-site radius, which is the result of substitution of La^{3+} by a larger Na^+ ion (radii 1.36 Å and 1.39 Å, respectively), is compensated by the decrease of the average Mn-site radius $<r_B>$ (as a result of partial oxidation of Mn^{3+} to smaller Mn^{4+} ions, radii 0.65 Å and 0.53 Å, respectively). Therefore, the unit cell volume of the perovskite structure remains constant for higher doping levels.

Tolerance factors and cation size mismatch for the Na doping levels studied in this work were calculated by using a 12-fold-coordinated ionic radius for the La site and a sixfold-coordinated ionic radius for the Mn site. The results are given in Table I.

Further, the rate of change of the cation size mismatch, σ^2, decreased for $x > 0.20$.

The surface morphology of the samples was investigated by use of SEM. For brevity, only two typical SEM images (magnification ×1000) of the samples with $x = 0.10$ and $x = 0.25$ are given in Fig. 2. Tightly connected grains are seen and the average grain size is nearly 5 μm for $x \leq 0.10$. As the Na concentration was increased grain size also increased, up to 30 μm. These large grains are more tightly bound, but inter-granular voids are also observed on the surfaces of samples with $x > 0.20$.

Field-cooled, temperature-dependent magnetization measurements were obtained in the range 100–320 K with an applied field of 100 Oe; the results were given in Fig. 3. These curves are typical paramagnetic–ferromagnetic phase transition curves. The T_C values were found to be approximately 150, 210, 280, 310, 260, 250, and 230 K for systematically increasing Na concentration. It is seen that T_C increases with increasing Na for concentrations up to $x = 0.20$, but then starts to decrease for Na concentrations $x > 0.20$. There could be several reasons for such behavior, including oxygen non-stoichiometry (excess or deficient oxygen), a change in Mn–O bond length and Mn–O–Mn bond angle, unit cell volume for a given crystal structure, and Mn^{4+}-to-Mn^{3+} ratio. It is well known that the presence of ferromagnetism (associated with electrical conduction) in the La-site-doped $LaMnO_3$ perovskite manganites is related to the double exchange (DE) mechanism which is favored when the Mn^{+4}-to-Mn^{+3} ratio is approximately 0.5, because the number of Mn^{4+}–O–Mn^{3+} chains in the structure that can contribute to DE maximized.[15] A formula for the deviation of this ratio from 0.5, can be derived as $\delta = |0.5 - Mn^{4+}/Mn^{3+}|$. For substitution with a monovalent ion, for example Na^+, this formula becomes $\delta = |0.5 - 2x/(1 - 2x)|$; in Fig. 4 δ this is plotted as a function of x ranging from 0.0 to 0.35. It is apparent that $\delta = 0.0$ for $x = 0.167$, which is the favored monovalent doping level for the DE mechanism. This would explain why T_C is maximum at x near 0.20, as seen in Fig. 4. It should be noted that, being a monovalent ion, Na^+ oxidizes two neighboring Mn^{3+} ions in close proximity to itself to two Mn^{4+} ions, yielding an extra increase in the probability of a competing super-exchange (SE) process as compared with divalent ion substitution.[16]

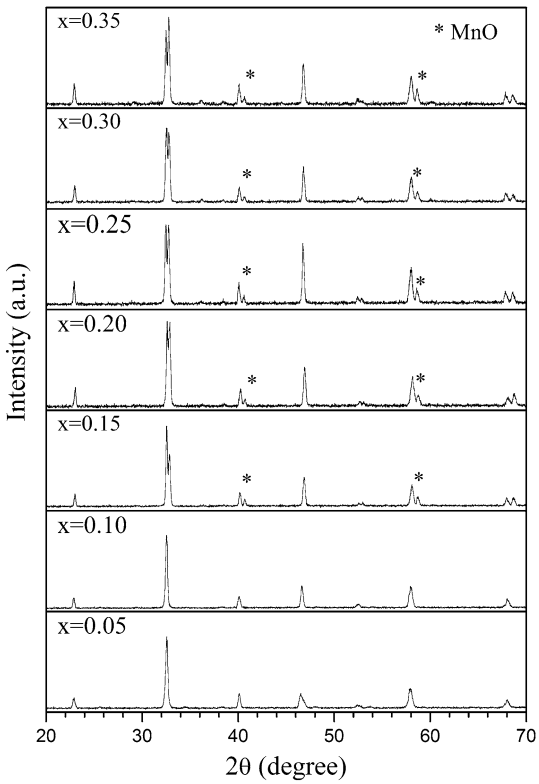

Fig. 1. XRD patterns of samples with different Na concentration sintered at 1400°C.

The temperature dependence of resistance of the samples was also measured in 100–320 K range, by use of a closed cycle helium cryostat, to investigate the change in the resistivity of the compounds with doping concentration. The resistivity of the samples was determined by use of the standard four-point probe technique. Figure 5 shows the normalized $\rho - T$ curves, which are indicative of typical metal–insulator behavior. The metal–insulator transition temperatures, T_{IM}, were calculated by taking the derivative of $\rho(T)$ w.r.t. temperature, and are given in Fig. 4 for comparison with T_C and δ. As expected from Zener's DE theory, the paramagnetic–ferromagnetic transition should be associated with the insulator–metal transition. The $La_{(1-x)}Na_xMnO_3$

Table I. Calculated lattice constants, unit cell volumes, and refinement data

x	t	σ^2	a (Å)	b (Å)	c (Å)	V (Å^3)	χ^2	R_p (%)	R_{wp} (%)
0.05	0.9603	0.0428	5.5398	5.5237	7.8136	239.0972	2.11	1.40	1.79
0.10	0.9662	0.0810	5.5275	5.5146	7.7964	237.6485	1.74	1.16	1.08
0.15	0.9723	0.1148	5.4827	5.5265	7.7723	235.5000	2.08	0.17	0.22
0.20	0.9784	0.1440	5.4659	5.5133	7.7672	234.0659	4.11	0.30	0.29
0.25	0.9846	0.1688	5.4712	5.5295	7.7287	233.8164	2.43	3.76	4.41
0.30	0.9909	0.1890	5.4757	5.5327	7.7379	234.4195	2.68	3.35	3.26
0.35	0.9972	0.2048	5.4633	5.5311	7.7237	233.3982	2.48	3.53	3.24

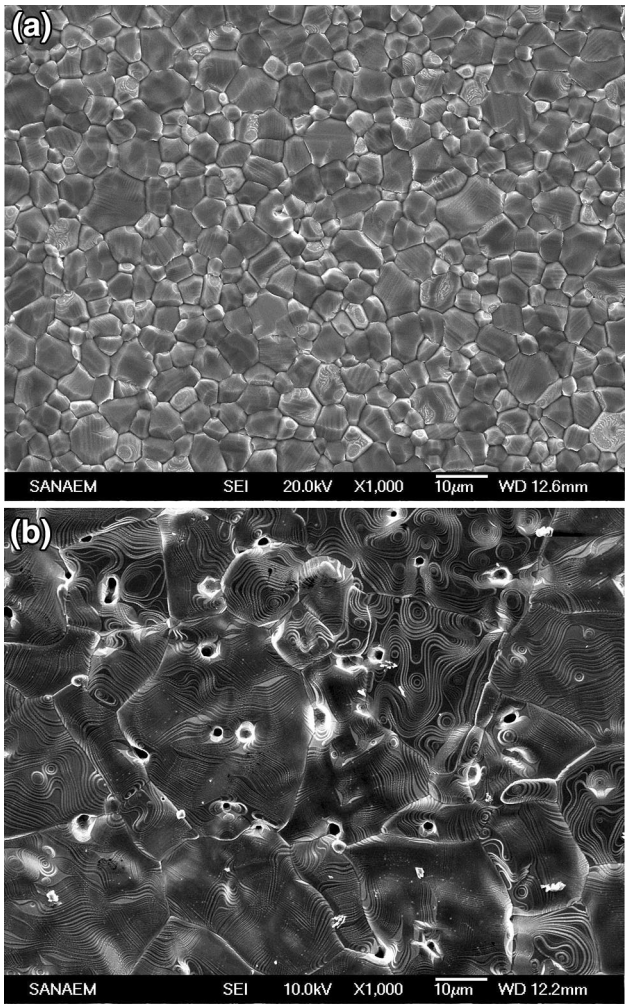

Fig. 2. SEM images of the samples: (a) $La_{0.90}Na_{0.10}MnO_3$; (b) $La_{0.75}Na_{0.25}MnO_3$.

studied in this work has very close T_C and T_{IM} temperatures, supporting the DE mechanism. Similar studies with Na doped perovskite manganites were conducted by Roy et al.,[5] Lakshmi et al.,[17] and Shivakumara et al.[18] In contrast with our results, the values reported for T_C and T_{IM} do not follow the same trend. For comparison with our result, their T_C and T_{IM} values were plotted and are presented in Figs. 6 and 7, respectively. The trend observed in T_C with increasing Na concentrations up to $x = 0.20$ was also observed in the studies performed by Roy et al.[5] and Lakshmi et al.[17] The difference between our results and theirs is the trend of T_C when the Na content is $x > 0.20$. Roy et al. and Lakshmi et al. explained the saturation of T_C for $x > 0.20$ on the basis of completion of the rhombohedral phase, which contributes to magnetization, development of the orthorhombic phase, which hinders magnetization, and domination of the SE interaction over the DE interaction with increasing Mn^{4+}-to-Mn^{3+} ratio. As stated above, substitution with the Na^+ ion causes an increase in $<r_A>$ and a decrease in $<r_B>$.

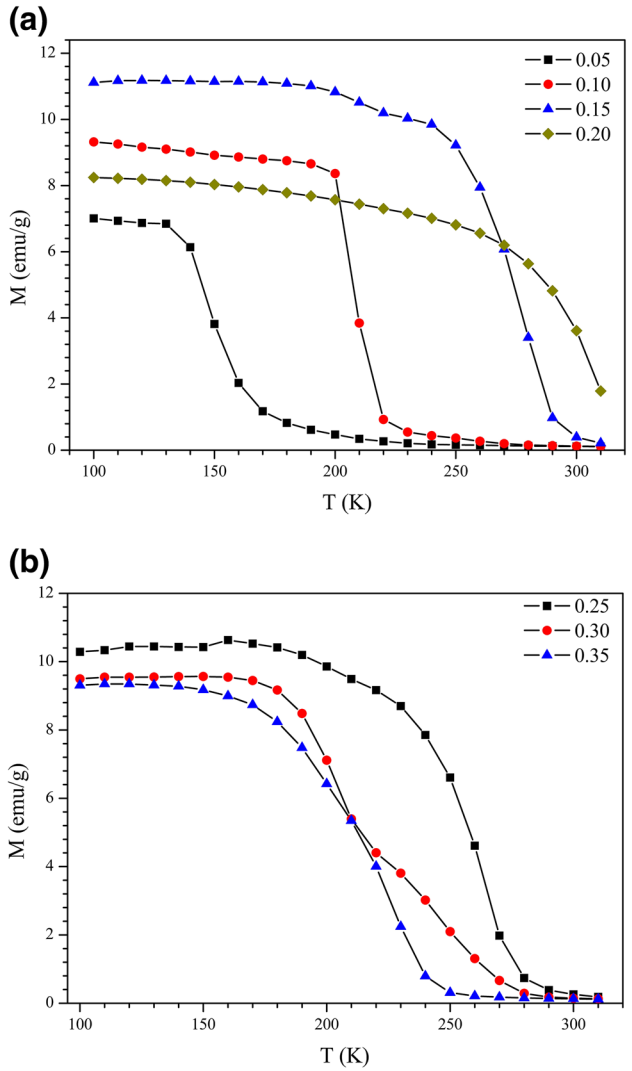

Fig. 3. Temperature dependence of magnetization of the samples.

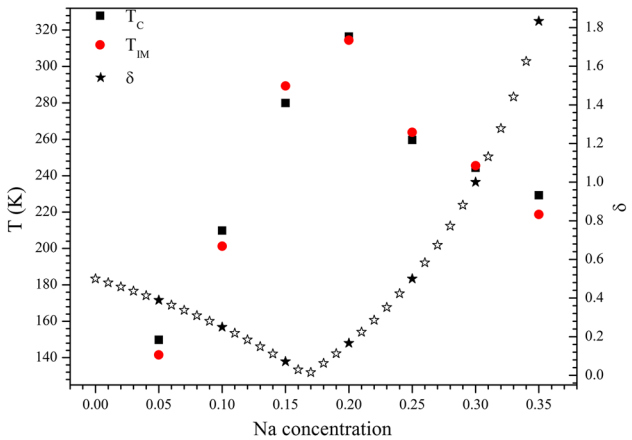

Fig. 4. $\delta = |0.5 - Mn^{4+}/Mn^{3+}|$. ratio deviation from 0.5, T_C, and T_{IM}.

The rate of change of $<r_B>$ is higher than that of $<r_A>$. An increase in $<r_A>$ and a decrease in $<r_B>$ possibly induce an increase of the average

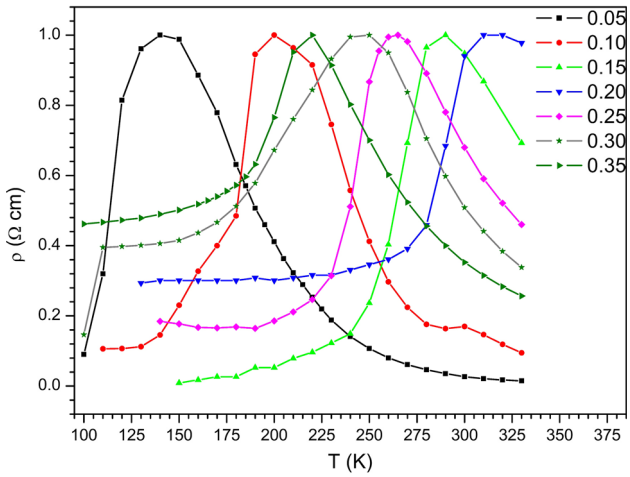

Fig. 5. Normalized resistivity w.r.t. temperature for different Na concentrations.

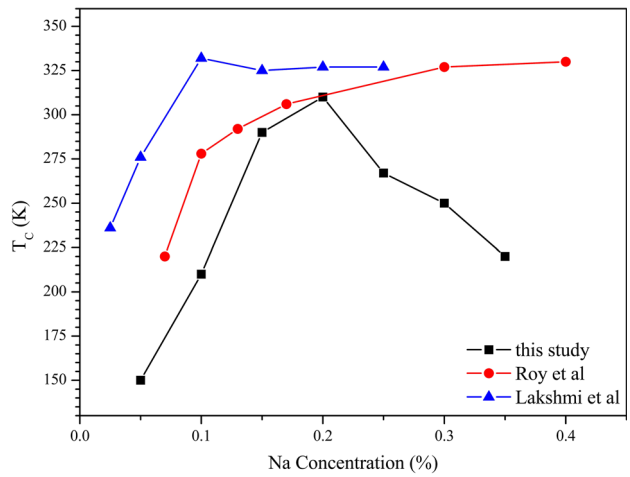

Fig. 6. Comparison of T_C in this work with literature reports.

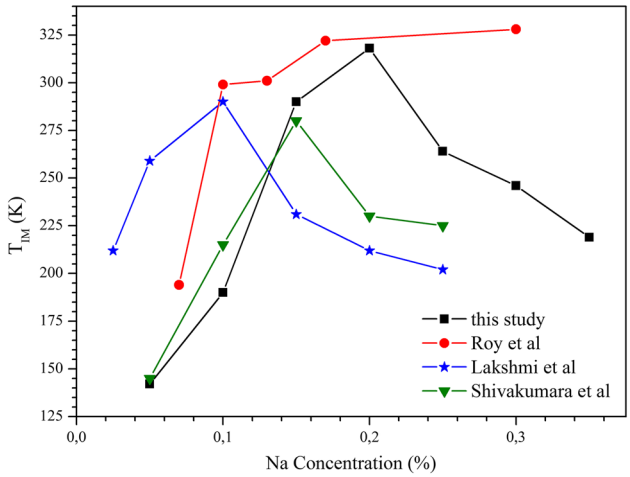

Fig. 7. Comparison of T_{IM} in this work with literature reports.

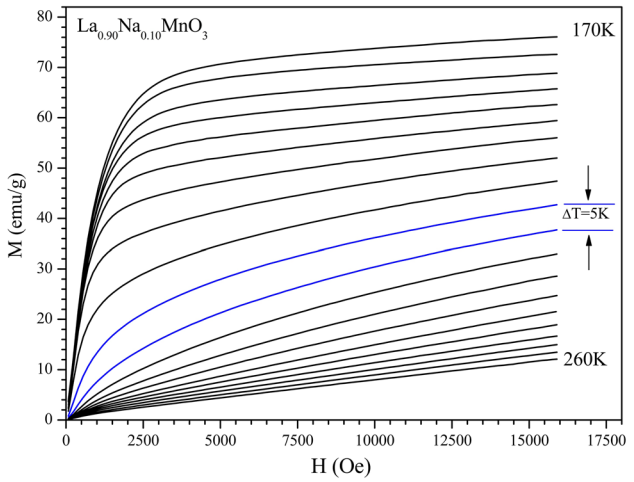

Fig. 8. Field dependent magnetization isotherms of $La_{0.90}Mn_{0.10}O_3$.

<Mn–O> bond length. Hence, the decrease of T_C in our work for $x > 0.20$ can be explained as follows. According to DE theory, an increase in Mn–O bond length corresponds to a decrease in Mn–O–Mn bond angle, which leads to weakening of the DE interaction and results in lowering of T_C. The rate of change of T_{IM} with x for Na-doped $LaMnO_3$ is the same as for other studies reported in the literature.[5,17,18] However, the values of T_{IM} are different for corresponding doping values, possibly because of the different sample-preparation conditions.

The isothermal magnetization curves for the sample with x = 0.10 are shown in Fig. 8.

The other samples have similar magnetization. These families of curves were taken with 5 K intervals, from approximately 50 K below T_C to approximately 50 K above, with external applied magnetic fields between 0 and 1.6 T. By using these isothermal magnetization measurements, we calculated the magnetic entropy changes (ΔS_M) for a maximum magnetic field (H) change of 1.6 T, on the basis of one of the thermodynamic equations of Maxwell, given below:

$$\Delta S_M(T, H_{max}) = S_M(T, H_{max}) - S_M(T, 0) = \int_0^{H_{max}} \left(\frac{\partial M}{\partial T}\right)_H dH \quad (1)$$

where M and T are magnetization and temperature, respectively. In the calculation of $\Delta S_M(T, H_{max})$, numerical approximation of the above integral was applied as follows:

$$|\Delta S_M(T, H_{max})| = \sum_j \left(\frac{M_i - M_{i+1}}{T_{i+1} - T_i}\right)_j \Delta H_j \quad (2)$$

where M_i and M_{i+1} are the experimental magnetization values obtained at temperatures T_i and T_{i+1} in a magnetic field H_j.

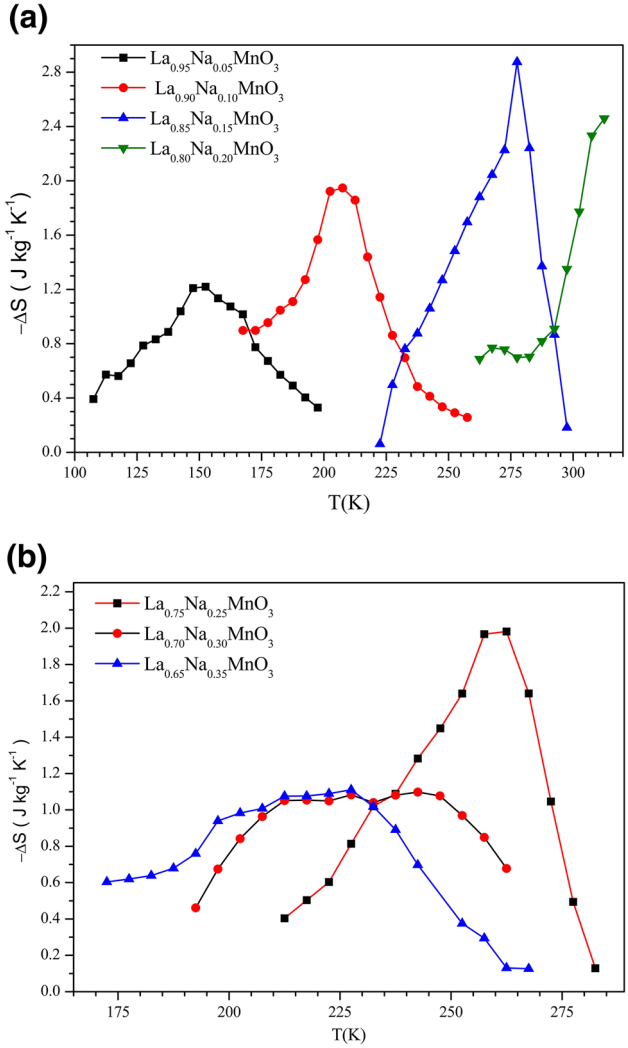

Fig. 9. Magnetic entropy changes of the samples w.r.t temperature under a magnetic field change of 1.6 T: (a) $x = 0.05$–0.20; (b) $x = 0.25$–0.35.

The calculated magnetic entropy changes w.r.t. temperature for different Na concentrations are given in Fig. 9. The maximum entropy changes were calculated to be 1.2, 1.85, 2.85, 2.4, 2.0, 1.1, and 1.12 J/kg K, for increasing Na concentration. The optimum value of Na concentration lies between 0.15 and 0.20 for high T_C and high magnetic entropy change. The compound obtained by doping with 20% Na may have potential for room-temperature applications.

CONCLUSION

We investigated, in detail, the structural, electrical, and magnetic properties of sol–gel-prepared $La_{(1-x)}Na_xMnO_3$ sintered at 1400°C with different Na concentrations from $x = 0.05$–0.35. It was observed that with a minor MnO impurity phase, the orthorhombic Pbnm crystal structure is maintained throughout the Na concentration range $0.05 \le x \le 0.35$, but that the unit cell volume of the compounds is inversely proportional to Na concentration up to 20%. Grain size also depends on Na concentration, ranging from 5–30 μm. Na concentrations above $x = 0.20$ lead to porous and pinhole like structures. T_C increases with increasing Na concentrations up to $x = 0.20$ but start to decrease for $x > 0.20$. The maximum magnetic entropy change increases with increasing Na content up to $x = 0.15$; the increase then ceases for further Na substitution. However, optimum T_C and ΔS_M values for room-temperature applications can be obtained when Na concentrations are between 0.15 and 0.20, when the Mn^{4+}-to-Mn^{3+} ratio is optimized, enabling more electrons to hop between neighboring Mn ions.

REFERENCES

1. Z.B. Guo, Y.W. Du, J.S. Zhu, H. Huang, W.P. Ding, and D. Feng, *Phys. Rev. Lett.* 78, 1142 (1997).
2. A. Das, M. Sahana, S.M. Yusuf, L. Madhav Rao, C. Shivakumara, and M.S. Hegde, *Mater. Res. Bull.* 35, 651 (2000).
3. A. Maignan, S. Hébert, L. Pi, D. Pelloquin, C. Martin, C. Michel, M. Hervieu, and B. Raveau, *Cryst. Eng.* 5, 362 (2002).
4. L. Pi, M. Hervieu, A. Maignan, C. Martin, and B. Raveau, *Solid State Commun.* 126, 229 (2003).
5. S. Roy, Y.Q. Guo, S. Venkatesh, and N. Ali, *J. Phys. Condens. Matter* 13, 229 (2001).
6. P. Ramirez, *J. Phys. Condens. Matter* 9, 8171 (1997).
7. M. Battabyal and T.K. Dey, *Phys. B Phys. Condens. Matter* 367, 40 (2005).
8. M.H. Phan and S.C. Yu, *J. Magn. Magn. Mater.* 308, 325 (2007).
9. Y. Xu, M. Meier, P. Das, M.R. Koblischka, and U. Hartmann, *Cryst. Eng.* 5, 383 (2002).
10. G. Tang, Y. Yu, W. Chen, and Y. Cao, *Mater. Lett.* 62, 2914 (2008).
11. X. Xiao, S.L. Yuan, Y.Q. Wang, G.M. Ren, J.H. Miao, G.Q. Yu, Z.M. Tian, and S.Y. Yin, *Solid State Commun.* 141, 348 (2007).
12. L.M. Rodriguez-Martinez, H. Ehrenberg, and J.P. Attfield, *Solid State Sci.* 2, 11 (2000).
13. L.W. Lei, Z.Y. Fu, and J.Y. Zhang, *Mater. Lett.* 60, 970 (2006).
14. Q. Xu, D. Huang, W. Chen, J. Lee, B. Kim, H. Wang, and R. Yuan, *Ceram. Int.* 30, 429 (2004).
15. J.B. Goodenough, *Annu. Rev. Mater. Sci.* 28, 1 (1998).
16. E. Taşarkuyu, A.E. Irmak, A. Coskun, and S. Aktürk, *J. Alloys Compd.* 588, 422 (2014).
17. Y.K. Lakshmi, G. Venkataiah, and P.V. Reddy, *J. Appl. Phys.* 106, 023707 (2009).
18. C. Shivakumara, M.B. Bellakki, A.S. Prakash, and N.Y. Vasanthacharya, *J. Am. Ceram. Soc.* 90, 3852 (2007).